

McDonald, J.J., Tay, D., Prime, D. J., & Hillyard, S. A. (in press). Isolating the neural substrates of visually guided attention orienting in humans. *Journal of Neuroscience*. <https://doi.org/10.1523/JNEUROSCI.0205-22.2022>

**Title:** Isolating the neural substrates of visually guided attention orienting in humans

**Abbreviated title:** Isolating visual orienting activity in humans

John J. McDonald<sup>1\*</sup>, Daniel Tay<sup>1</sup>, and David J. Prime<sup>1</sup>, Steven A. Hillyard<sup>2,3</sup>

<sup>1</sup>Department of Psychology, Simon Fraser University, Burnaby, BC, Canada, V5A 1S6

<sup>2</sup>Department of Neurosciences, University of California San Diego, 9500 Gilman Drive, La Jolla, California, 92093

<sup>3</sup>Leibniz Institute for Neurobiology, Magdeburg, Germany

\*Corresponding author's Email: [jmcd@sfu.ca](mailto:jmcd@sfu.ca)

#### **Acknowledgements**

We thank John Gaspar for help with Experiment 2 of this paper, Jessica J. Green for assistance with the flicker-fusion task, and several lab members for assistance in data collection. This study was supported by the Natural Sciences and Engineering Research Council of Canada, the Canadian Foundation for Innovation, and the Canada Research Chairs program. The authors declare no competing financial interest.

Dave Prime is now at the Department of Psychology, Douglas College, New Westminster, BC, Canada

**Conflict of Interest:** The authors declare that there were no competing conflicts of interest.

**Author Contributions:** J.J.M., D.T., and D.J.P. designed the research; D.T., and D.J.P. performed the research; J.J.M, D.T., and D.J.P. analyzed data; All authors wrote the paper.

#### **Manuscript details:**

Number of pages: **38**

Number of figures (**6**), tables (0), multimedia (0), and 3D models (0)

Number of words in Abstract (**170**), Introduction (**647**), and Discussion (**1485**)

**Abstract**

The neural processes that enable healthy humans to orient attention to sudden visual events are poorly understood because they are tightly intertwined with purely sensory processes. Here we isolated visually guided orienting activity from sensory activity using scalp-recorded event-related potentials (ERPs). By recording ERPs to a lateral stimulus and comparing waveforms obtained under conditions of attention and inattention, we identified an early positive deflection over the ipsilateral visual cortex that was associated with the covert orienting of visual attention to the stimulus. Across five experiments, this ipsilateral visual orienting activity (VOA) could be distinguished from purely sensory-evoked activity and from other top-down spatial attention effects. The VOA was linked with behavioral measures of orienting, being significantly larger when the stimulus was detected rapidly than when it was detected more slowly, and its presence was independent of saccadic eye movements towards the targets. The VOA appears to be a specific neural index of the visually guided orienting of attention to a stimulus that appears abruptly in an otherwise uncluttered visual field.

**Keywords:** covert orienting, attention, abrupt visual onset, event-related potentials, visual orienting activity (VOA)

**Significance Statement**

The study of visual attention orienting has been an important impetus for the field of cognitive neuroscience. Seminal reaction-time studies demonstrated that a suddenly appearing visual stimulus attracts attention involuntarily, but the neural processes associated with visually guided attention orienting have been difficult to isolate because they are intertwined with sensory processes that trigger the orienting. Here, we disentangled orienting activity from sensory activity using scalp recordings of event-related electrical activity in the human brain. A specific neural index of visually guided attention orienting was identified. Surprisingly, whereas peripheral sensory stimulation is processed initially and predominantly by the contralateral visual cortex, this electrophysiological index of visual orienting was recorded over the cerebral hemisphere that was ipsilateral to the attention-capturing stimulus.

## Introduction

Visual stimuli that appear suddenly often interrupt ongoing performance to become the focus of one's awareness. Such stimulus-driven changes in awareness have been discussed in terms of the orienting of attention for over a century (James, 1890; Hatfield, 1998). Contemporary cognitive psychologists have hypothesized that observers orient their attention involuntarily to abruptly appearing visual stimuli and that such stimuli capture attention even when they are irrelevant to the task at hand (Posner, 1980; Yantis and Jonides, 1990; Egeth and Yantis, 1997). In neuroscientific terms, an abruptly appearing visual stimulus is hypothesized to trigger a cascade of attention-control operations that ultimately brings attention to bear upon the stimulus, even if there is no overt change in the observer's direction of gaze (Posner and Petersen, 1990; LaBerge, 1995; Corbetta and Shulman, 2002).

Research in non-human primates has begun to distinguish neural activities associated with the stimulus-driven orienting of attention from sensory responses at the level of the individual neuron. Many neurons in the lateral intraparietal area and superior colliculus were shown to respond initially to the abrupt appearance of a visual stimulus in their receptive fields and again immediately before the animal makes a saccadic eye movement to the stimulus (Wurtz and Goldberg, 1972; Duhamel et al., 1992; Rodgers et al., 2006; Marino et al., 2008). The initial transient responses reflect not only the passive sensory registration of the stimulus but also representations of stimulus priority that trigger orienting (Boehnke and Munoz, 2008; Bisley et al., 2011). The neural processes that enable stimulus-driven orienting in humans have yet to be identified, however, in part because it is difficult to disentangle the orienting processes from sensory processes. This difficulty, which applies equally to neurophysiological recordings (e.g., event-related brain potentials; ERPs) and to neuroimaging methods (e.g., fMRI), has been a major impediment to the investigation of stimulus-driven covert orienting in healthy humans.

Our aim was to isolate neural activity associated with visually guided orienting in humans using EEG-based measures. The first step was to consider prototypical occipital ERP waveforms elicited by a lateral, attention-capturing visual stimulus (**Fig. 1**). Waveforms recorded from the posterior scalp contralateral and ipsilateral to the stimulated visual hemifield include an initial

positive voltage peak (P1) and a subsequent negative voltage peak (N1) (Luck and Hillyard, 1994a; Mangun, 1995; Di Russo et al., 2002). The P1 first appears over the contralateral scalp (peaking 100–120 ms post-stimulus) because of the contralateral projections from retina to occipital cortex. After a ~20-ms delay, a similar P1 is elicited over the ipsilateral scalp by way of the callosal fibres that connect the two cortical hemispheres (Mangun, 1995). The N1 typically unfolds in the same manner, peaking first contralaterally and then ipsilaterally. The contralateral and ipsilateral peaks also differ in amplitude: the P1 is generally largest over the ipsilateral scalp, whereas the N1 is largest over the contralateral scalp.

The contralateral-ipsilateral differences shown in **Fig. 1** have long been considered to be purely sensory consequences of the lateralized stimulation and not indicative of attentional orienting (Luck and Hillyard, 1994a; Rugg et al., 1984; Saron and Davidson, 1989; Stormer et al., 2019). Although this sensory interpretation has rarely been questioned, it is possible that attentional processes also contribute to the lateralized differences (Wascher and Beste, 2010; Yamaguchi et al., 1994). Here, we present a series of experiments that aimed to isolate orienting-related activity from purely sensory activities. The main strategy was to compare ERPs elicited by a lateral, abrupt-onset visual stimulus when the task required participants to orient their attention towards the stimulus or away from it. Our approach was novel in that it focused on attention-orienting activity itself rather than on the effects of having previously oriented attention to a particular location on the processing of stimuli appearing there or elsewhere (e.g., Van Voorhis and Hillyard 1977; Eimer, 1994b; Mangun and Hillyard, 1991; Hopfinger and Mangun, 1998; Di Russo et al. 2003). These previous studies of spatially focused attention have demonstrated that visual stimuli appearing at an already attended location elicit larger P1 and/or N1 components than do stimuli at an unattended location but do not provide information on the ERP modulations associated with the actual orienting or directing of attention *per se*.

## **Materials and Methods**

The Research Ethics Board at Simon Fraser University approved the research protocol used in this study.

**Participants.** Undergraduate students from Simon Fraser University were recruited to participate in the experiments reported within. After giving informed consent, 19 students participated in Experiment 1, 12 students participated in Experiment 2, 24 students participated in Experiment 3, 31 students participated in Experiment 4, and 36 students participated in Experiment 5. The students were given course credits as part of a departmental research participation system. Participant data were excluded from analysis if more than 30% of trials were contaminated by ocular artifacts (rejection criterion set in advance). Data from 30 participants were excluded in total (three from Experiment 1, seven from Experiment 3, seven from Experiment 4, and 12 from Experiment 5). All of the remaining participants had normal color vision and normal or corrected-to-normal visual acuity (Experiment 1: information on participants' sex, handedness, and age were lost as a result of a flood; Experiment 2: 11 females, 11 right-handed, mean age: 20.1 years; Experiment 3: 15 females, 16 right-handed, mean age: 20.6 years; Experiment 4: 20 females, 21 right-handed, mean age: 20.9 years; Experiment 5: 19 females, 23 right-handed, mean age: 18.5 years).

**Apparatus.** All experiments were conducted in an electrically shielded and sound-attenuated chamber dimly illuminated by DC-powered LED lighting. Visual stimuli were presented on a 19-inch CRT monitor (Experiment 1) or a 23-inch, 120-Hz LCD monitor that was viewed from a distance of 57 cm. Stimulus presentation was controlled by Presentation (Neurobehavioral Systems, Inc., Albany, CA) from a Windows-based computer. EEG was recorded using custom software (Acquire) from a second, Windows-based computer, using a 64-channel A-to-D board (PCI 6071e, National Instruments, Austin, TX) connected to a high input impedance EEG amplifier system (SA instruments, San Diego, CA).

**Stimuli and procedure. *Brightness matching.*** In Experiment 2, the flicker-fusion procedure (Ives, 1912) was used to ensure that the red line was perceptually isoluminant with the grey background. A  $11^\circ \times 11^\circ$  grey square and a same-size red square were presented alternately at the same location at 60 Hz. Each participant viewed the flickering image freely and adjusted the luminance of the red square until minimal flicker was perceived. This procedure was

performed twice to yield two sets of RGB values. The average of the RGB values was computed separately for each participant and was used for the red line.

In Experiments 3–5, a modified method-of-limits procedure was used to psychophysically match the perceived luminance of the red line and grey disc (Hickey et al., 2009). A grey, vertical rectangle ( $1.9^\circ \times 2.8^\circ$ ) of the same RGB value as the grey disc (109, 109, 109 in Experiment 3; 90, 90, 90 in Experiment 4) was presented next to a same-sized red rectangle on a black background. One of the rectangles was presented on the left and the other was presented on the right of the vertical meridian with equal probability. Participants viewed the display freely and adjusted the luminance of the red rectangle until the red was perceived to be equal in luminance with that of the grey rectangle. This matching procedure was repeated four times to yield four sets of RGB values, and the average of the RGB values was computed separately for each participant to color the red line in the target display. The grey rectangle had a fixed RGB value throughout the brightness-matching procedure, whereas the red rectangle had an initial luminance that is approximately  $3 \text{ cd/m}^2$  higher than the grey rectangle, and the red rectangle in subsequent brightness-matching displays had initial luminance that alternated in being approximately  $3 \text{ cd/m}^2$  lower or higher than the value obtained from the preceding match.

**Experiment 1.** Visual stimuli were presented on a black background. During the intertrial interval, three white, unfilled boxes ( $0.25^\circ \times 0.25^\circ$ ) were vertically stacked at the center of the display ( $0.5^\circ$  centre-to-centre spacing), and participants fixated their gaze on the middle of the three boxes. After 1350–1650 ms, a target display appeared for 750 ms. One segment from each fixation box disappeared at the onset of a target display. Two of the fixation boxes had either the left or right segment removed to reveal a C or mirror-reverse C shape, and the third box had the top or bottom segment removed to reveal a U or inverted U shape. The location of the U in the vertically stacked fixation stimuli was chosen randomly on each trial. Each target display also contained a notched red disc ( $2^\circ$  dia.;  $19 \text{ cd/m}^2$ ;  $x = 0.63$ ,  $y = 0.32$ ). The disc was equally likely to appear on the left or right side of fixation (coordinates within hemifield determined randomly), and the notch was equally likely to be shallow ( $0.5^\circ \times 0.5^\circ$ ) or deep ( $0.5^\circ \times 1.0^\circ$ ). In different halves of the experimental session, participants discriminated the depth of the lateral disc's notch (attend-

disc condition) or indicated whether the fixation stimuli included an upright or inverted U (fixation condition) by pressing one of two buttons of a computer mouse with their right hand. All participants were given at least one block of practice, during which feedback about eye position and blinking rate was provided. All participants were encouraged to blink infrequently during blocks and to take a short rest break between blocks. Participants completed 576 trials for each condition (order counterbalanced), with rest periods after 24 successive trials.

**Experiment 2.** Visual stimuli were presented on a grey background with one of two luminance levels. The lighter ( $74 \text{ cd/m}^2$ ) of the two served as the background for the fixation display, and the darker ( $16 \text{ cd/m}^2$ ) served as the background for the target display. A filled, black dot ( $0.2^\circ$  in diameter) persisted across the two displays to serve as a fixation point. On each trial, the fixation display appeared for 800–1200 ms and was then replaced by the target display, which lasted for 750 ms. The target display contained an isoluminant, red, horizontal line ( $0.7^\circ \times 0.1^\circ$ ) on half the trials (the remaining trials contained no red line). On line-present trials, the red line appeared in one of twelve, equally spaced locations around an imaginary circle (radius:  $4.2^\circ$ ) centered on fixation. None of these locations were on a meridian (vertical or horizontal). The line, which served as the target, varied in salience across two halves of the experiment (high salience:  $x = 0.63$ ,  $y = 0.32$ ; low salience:  $x = 0.35$ ,  $y = 0.32$ ; order counter-balanced across participants). Salience was varied by changing the proportions of red, green, and blue light of the line so that the redness would be more or less grey. Specifically, the RGB coordinates of the display background, salient line, and less-salient line were [110, 110, 110], [164, 0, 0], and [114, 86, 86], respectively. Target-present and target-absent trials were randomly intermixed within each block. Participants pressed one of two buttons depending on whether the target display contained a red line or not. Participants completed 30 blocks of 48 trials (15 blocks per salience level). All other procedures were identical to Experiment 1.

**Experiment 3.** A filled, black dot ( $0.3^\circ$  in diameter) was displayed continuously to serve as a fixation point. As in Experiment 2, the luminance of the grey background was lowered from a lighter level ( $74 \text{ cd/m}^2$ ) during the fixation period to a darker level ( $16 \text{ cd/m}^2$ ) during the target display. Target displays were identical to the high-salience-line displays in Experiment 2, except



for two differences. First, the line was short or long with equal probability (short:  $0.4^\circ \times 0.1^\circ$ ; long:  $0.7^\circ \times 0.1^\circ$ ). Second, a small notch appeared at the top of the otherwise filled fixation dot. The notch was either shallow ( $0.05^\circ \times 0.03^\circ$ ) or deep ( $0.05^\circ \times 0.1^\circ$ ). Each participant performed in two conditions, each with 15 successive blocks. In the attend-periphery condition, participants pressed one of two buttons to discriminate the length of the red line. In the attend-fixation condition, participants pressed one of two buttons to discriminate the depth of the fixation notch. Roughly half of the participants performed in the attend-periphery condition first while the rest performed the attend-fixation condition first. All other procedures were identical to Experiment 2.

**Experiment 4.** A filled, white dot ( $0.2^\circ$  in diameter) persisted across the fixation and target displays to serve as a fixation point. As in Experiment 3, the luminance of the grey background was lowered from a lighter level ( $35 \text{ cd/m}^2$ ) during the fixation period to a darker level during the target display. This time, however, the luminance of the target-display background was slightly darker within a circular region centered on the fixation point than it was outside of the circular region, giving the perception of a faint, grey disc (background:  $22 \text{ cd/m}^2$ ; disc:  $20 \text{ cd/m}^2$ ). On each trial, the radius of this grey disc was randomly determined to be  $6.25^\circ$  or  $7.5^\circ$  (described to participants as small or large) with equal probability. As in Experiment 3, each target display also contained a red, horizontal line at one of twelve possible locations  $4.2^\circ$  from fixation, so that it always appeared within the confines of the faint grey disc. In two different halves of the experimental session, participants either discriminated line length (attend-line condition) or disc size (attend-disc condition) and pressed one of two buttons accordingly. Each condition comprised of 12 contiguous blocks of 48 trials (order counterbalanced across participants). All other procedures were identical to Experiment 3.

**Experiment 5.** The stimuli and procedure were identical to those used in Experiment 4 except as follows. The disc in the display was darker ( $11 \text{ cd/m}^2$ ), appeared in one of three sizes (radii:  $11.0^\circ$ ,  $12.4^\circ$ , and  $13.8^\circ$ ), and was absent on half the trials. On disc-absent trials, the background luminance decreased to that of the disc. On disc-present trials, the background had a luminance level of  $22 \text{ cd/m}^2$ , which was also the luminance of the grey background in the fixation interval. In the attend-line condition, participants discriminated the length of the red line as in

Experiment 3. But in the attend-disc condition, participants pressed one of two gamepad buttons to indicate whether the disc was present or absent (stimulus-response mapping counterbalanced across participants). Each condition comprised of 15 contiguous blocks of 48 trials (order counterbalanced across participants).

**Electrophysiological recording and analysis.** EEG signals were recorded with either 63 tin electrodes (in Experiments 1–3) or 24 Ag/AgCl electrodes (Experiments 4 and 5) housed in an elastic cap, using our standard lab procedures, including rejection of trials with ocular artifacts (Tay et al., in press). ERPs were computed from artifact-free epochs of EEG and electrooculographic (EOG) signals, separately for each condition within each experiment. The ERPs were further subdivided in Experiment 2 for target-present and target-absent displays and in Experiment 5 for disc-present and disc-absent displays. ERPs recorded contralateral and ipsilateral to the red stimuli constructed using conventional methods (by collapsing across left- and right-field stimuli and left and right hemisphere electrodes). Difference waves were computed by subtracting target-absent ERPs from target-present ERPs (separately for contralateral and ipsilateral waveforms; Experiment 2), attend-fixation-condition ERPs from attend-periphery-condition ERPs (Experiment 3), contralateral ERPs from ipsilateral ERPs (Experiment 4), and attend-disc-condition ERPs from attend-line-condition ERPs (Experiments 4 and 5).

All ERP measurements were taken from waveforms recorded at PO7 and PO8, because visually evoked peaks (P1 and N1) and attention-related components (e.g., N2pc) are typically largest at or near these electrodes (Luck and Hillyard, 1994a, 1994b; Mangun, 1995; Eimer, 1996; Luck et al., 1997; Hopf et al., 2000; Di Russo et al. 2002; Hickey et al., 2009). All statistical tests were two-tailed, paired  $t$  tests except for a one-sample test involving signed area, which is a directional test by its nature (e.g., signed positive area cannot be less than zero). Given the inherent difficulty in asserting the null hypothesis in conventional  $t$  tests, we computed the JZS Bayes Factor ( $BF$ ) using a scale  $r$  (Cauchy scale) value of .707 to corroborate those where the null was asserted (Rouder et al., 2009). We reported  $BF_{01}$  values to denote the relative likelihood of observing the data given the null hypothesis is true relative to observing the data given the alternative hypothesis is true. Component magnitudes were quantified using signed areas rather

than mean amplitudes because considerable variation in component timing was expected a priori. Unlike mean amplitudes, which must be measured in sufficiently narrow time windows, signed areas can be measured using wide windows that minimize problems arising from “cherry picking” (e.g., inflation of Type 1 error rate; Sawaki et al., 2012). The magnitude of the P1 was measured as the signed positive area in a 100-ms time window in Experiments 1–3. The width of this window was chosen to span the contralateral and ipsilateral peaks, and the start latency was tailored for the stimulus salience (Experiment 1: 50–150 ms; Experiment 2: 150–250 ms for high-salience targets and 175–275 ms for low-salience targets; Experiment 3: 150–250 ms; here and elsewhere, all times specified relative to onset of the target display). In Experiments 4 and 5, only the ipsilateral P1 (125–225 ms) was measured because early peaks driven by the display-wide luminance change overlapped with the contralateral P1. The magnitude of the N1 was measured as the signed negative area in a 100-ms time window that spanned the contralateral and ipsilateral peaks. The start latency was once again selected based on stimulus salience (Experiment 1: 125–225 ms; Experiment 2: 175–275 ms for high-salience targets; 200–300 ms for low salience targets; no measurement in Experiments 3–5 because most of the N1 activity were obscured by the overlapping P3 activity). The latencies of the various P1 and N1 peaks (contralateral and ipsilateral) were measured as the time point at which the ERP deflection reached 50% of its peak amplitude. These measures were taken where applicable (i.e., when peaks of both the contralateral and ipsilateral activity were observed). Differences in onset latencies were evaluated statistically using a conventional jackknife approach that replaces individual-subject data with N-1 sub-averages (and later correcting for the reduced variability; Miller et al., 1998). In Experiments 1 and 3, visual orienting activity (VOA) was isolated by subtracting ERPs obtained in the attend-fixation condition from analogous ERPs obtained in the attend-periphery condition.

In Experiments 4 and 5, all of the ERP measurements (aside from the ipsilateral P1 magnitudes) were based on the attend-line-condition-minus-attend-disc-condition difference waves that were used to isolate orienting activity. The VOA measurements were taken after the contralateral difference waveform was subtracted from the ipsilateral difference waveform. VOA

magnitude was computed as the signed positive area within a 100–250-ms window. The presence of VOA was tested using a nonparametric permutation approach that compared the measured signed area from a grand-averaged waveform to the signed area that would be expected in the complete absence of the signal (i.e., on the basis of noise alone; Sawaki et al., 2012). This was accomplished by randomly reassigning the side of the lateral stimulus (e.g., a left stimulus would be randomly reassigned as a left or right stimulus) and re-computing the grand-averaged ERPs. Such reassignment removes the lateralized ERP signal to enable computation of signed area due to noise on one permutation. This process was repeated 500 times to yield 500 permutations of the grand-averaged ERP. The signed positive areas obtained from these permutations were used to provide a distribution of values expected if a null hypothesis were true. In line with the traditional threshold for statistical significance, the observed grand-averaged ERP component was considered statistically present if the measured signed area fell beyond the 95<sup>th</sup> percentile of the estimated noise distribution. The  $p$  value for this permutation test was calculated using the following equation (Phypson and Smyth, 2010):

$$p = \frac{1 + (\text{number of permuted values} \geq \text{observed area})}{1 + \text{total number of permutations}}$$

Because the permutations test does not yield parametric measures, we followed the signed area analysis of VOA with a mean-amplitude analysis using a one-sample  $t$  test and then estimated the effect size using Cohen's  $d$ . The mean amplitude was measured in a 75-ms window that was contained within the 100–250 ms window used for signed area measurement. The 75-ms window was fitted to the VOA peak in the grand-average difference wave.

The difference waveform was separately computed for fast-response and slow-response trials, which were determined using a median split of RTs (McDonald et al., 2013). Split-half reliability of the VOA was computed by sorting alternating trials into two different averaging bins (separately for each condition), re-constructing difference waves separately for the two halves of trials for each participant, re-measuring the signed positive area for each half, and computing the Spearman-Brown coefficient between the areas measured from the split halves.

VOA onset latency was defined as the time at which the deflection reached 50% of its peak amplitude (again using Jackknife sub-averages in place if individual subjects). The VOA onset latency was compared with the onset latency of HEOG deflection averaged from trials wherein an eye-movement artifact was detected (i.e., unrestrained saccades). Onset latency of HEOG deflection was also defined as the time at which this activity first reached 50% of its peak, using jackknife sub-averages.

Topographical voltage maps of the ERP waveforms were constructed by spherical spline interpolation (Perrin et al., 1989). Maps of the target-elicited ERPs in Experiment 2 were plotted after subtracting ERP activity recorded on target-absent trials (i.e., present-absent difference wave). In Experiment 3, a map of the VOA was plotted after subtracting ERPs in the attend-fixation condition from ERPs in the attend-periphery condition. In Experiments 4 and 5, maps were plotted after subtracting ERPs in the attend-disc condition from ERPs in the attend-line condition (i.e., attend-line-minus-attend-disc difference). All maps were created by collapsing over left and right targets and left and right electrodes such that electrodes on the left and right sides were ipsilateral and contralateral to the eliciting stimulus, respectively.

Neural sources of the attend-periphery-minus-attend-fixation difference waveforms from Experiments 1 and 3 were modeled in BESA (version 6.1). The difference-wave activities were modelled using three discrete regional sources in the time range of the VOA (Experiment 1: 150–190 ms; Experiment 3: 190–240 ms). Two of the regional sources accounted for the positivities over the ipsilateral and contralateral occipital scalp, while the third regional source accounted for anterior negativities. Each source was added successively, with the first, second, and third sources ending up in ipsilateral occipital cortex (primary source), contralateral occipital cortex, and frontal cortex, respectively. No further sources were added to the model because a principal component analysis (PCA) of the residual waveforms yielded no dominant component. The coordinates of each source were estimated using BESA's standardized finite element model (for adults) and then related to known anatomy using an online tool (the MNI <-> Talaraich Tool; BiImage Suite Web).

## Results

In Experiment 1, the lateral stimulus appeared on a black background simultaneously with no-onset fixation stimuli that were revealed by removing one segment of each of the three fixation boxes (**Fig. 2A**). With this design, observers would perceive the disc to appear abruptly and the three-sided fixation stimuli to appear simultaneously with no new onset (Yantis and Jonides, 1984). Although we examined the prominent P1 and N1 peaks in each condition (**Fig. 2B**), the main goal was to isolate visually guided orienting activity (VOA) by subtracting the target-display ERPs obtained in the attend-fixation condition from the target-display ERPs obtained in the attend-periphery condition (**Fig. 2C–E**).

As expected, the P1 occurred earlier over the contralateral scalp than the ipsilateral scalp in both conditions [attend-fixation: 74 ms vs. 106 ms,  $t(15) = 6.25$ ,  $p < .001$ ,  $d = 2.18$ ; attend-periphery: 78 ms vs. 108 ms,  $t(15) = 9.26$ ,  $p < .001$ ,  $d = 2.56$ ]. The same was true for the subsequent N1 peak, although the timing differences were not as large as for the P1 [attend-fixation: 138 ms vs. 153 ms,  $t(15) = 2.27$ ,  $p = .038$ ,  $d = 0.65$ ; attend-periphery: 142 ms vs. 162 ms,  $t(15) = 4.51$ ,  $p < .001$ ,  $d = 1.23$ ]. In contrast, the only contralateral-vs.-ipsilateral amplitude difference to be found significant was that of the N1 measured in the attend-periphery condition. In that condition, the contralateral N1 (area over 125–225 ms:  $-256 \mu\text{V}\cdot\text{ms}$ ) was larger than the ipsilateral N1 ( $-140 \mu\text{V}\cdot\text{ms}$ ),  $t(15) = 3.80$ ,  $p = .002$ ,  $d = 0.65$ . Because the sensory stimulation was identical across conditions, we conclude that the disc triggered neural activity above and beyond purely sensory processing when it was designated as the target. Importantly, the amplitude of the ipsilateral N1 varied across conditions,  $t(15) = 5.49$ ,  $p < .001$ ,  $d = 0.89$ , but the amplitude of the contralateral N1 did not,  $t(15) = 0.48$ ,  $p = .636$ ,  $BF_{01} = 3.54$ . Thus, it appears that the attention-related process indexed by the lateralized amplitude difference occurred predominantly in the ipsilateral cortex and was manifest as an enhanced ipsilateral positivity (or alternatively, as a reduction of ipsilateral negativity) over the interval 125–225 ms when the abrupt-onset stimulus was attended.

**Fig. 2C** shows the attend-periphery-minus-attend-fixation difference waves at contralateral and ipsilateral occipital scalp locations (electrodes PO7 and PO8). Approximately 125 ms after display onset, the ipsilateral waveform became more positive than the contralateral waveform.

This positive difference is designated as Visual Orienting Activity (VOA). The initial phase of this difference corresponded to the amplitude reduction of the ipsilateral N1 in the attend-periphery condition. Within that time range, the topography of the attend-periphery-minus-attend-fixation difference clearly shows a positive voltage peaking over the ipsilateral occipital scalp (**Fig. 2D**). No amplitude difference was seen in the time range of the P1.

The neural sources of the difference-wave activity were modeled in BESA (version 6.1) using three discrete regional sources to provide converging evidence for the ipsilateral nature of the VOA. One regional source located along the lingual gyrus of the ipsilateral occipital cortex (Talairach coordinates:  $x = -32.6$ ,  $y = -76.7$ ,  $z = -4.2$ ) accounted for over 90% of the difference-wave distribution over the 150–190-ms interval, including the ipsilateral VOA. Other, less active regional sources in contralateral occipital cortex ( $x = 39.3$ ,  $y = -84.0$ ,  $z = -10.7$ ) and frontal cortex ( $x = 28.8$ ,  $y = 7.8$ ,  $z = 30.3$ ) accounted for the very small posterior contralateral positivity and an anterior negativity, respectively. The full three-source model accounted for over 96% of the activity within the 150–190-ms interval. A PCA of the residual activity revealed no dominant principal component, and so no additional source was added.

The results of Experiment 1 indicate that it is possible to isolate visually guided orienting activity from purely sensory activities and suggest that the VOA is a signature of visually guided covert orienting of attention. Surprisingly, the VOA was localized almost exclusively to the ipsilateral visual cortex rather than the contralateral visual cortex. However, such conclusions cannot be made unequivocally on the basis of Experiment 1 alone without further evaluating low-level sensory contributions to, and other alternative explanations for, the VOA. Accordingly, we developed a novel stimulus presentation method in an attempt to completely eliminate lateral sensory imbalance. Although such sensory imbalance was found to persist, the new method enabled us isolate visual orienting activity from purely sensory activity and rule out alternative explanations for the VOA. In what follows, we will demonstrate that the VOA is a newly discovered brain signal of spatial attention that originates primarily from the ipsilateral visual cortex.

The new stimulus presentation method that was developed utilized a change in background luminance at the moment a lateral abrupt-onset stimulus appeared. This stimulus-presentation method was used in Experiments 3–5 to isolate the VOA and to rule out alternative explanations for the orienting activity. We first conducted Experiment 2 to confirm that a lateral stimulus would elicit delayed but otherwise prototypical P1 and N1 components in the presence of a uniform, display-wide luminance change (brightness matched to stimulus using a flicker-fusion method; Ives, 1912). Wijers et al. (1997) showed that the P1 and N1 components are delayed by as much as 50 milliseconds when a stimulus appears on an isoluminant background (vs. non-isoluminant background). Such a delay in sensory processing would enable us to determine whether the orienting activity was closely tied to the timing of the sensory-evoked componentry (P1 and N1). To further vary the timing of the P1 and N1, the salience of the target was manipulated across high- and low-salience blocks. This was motivated, in part, on prior work showing that stimulus luminance modulates the timing and amplitude of the P1 and N1 peaks (Johannes et al., 1995). Participants (N = 12) were instructed to indicate whether the red line was present or absent when the luminance change occurred.

The results of Experiment 2 are shown in **Fig. 3**. On target-absent trials, the display-wide luminance change elicited a negative deflection that peaked at 68 ms over the dorsal parietal scalp and a positive deflection that first peaked at 106 milliseconds with amplitude maxima over the midline occipital scalp (**Fig. 3B**, top). These deflections were evident (with reduced amplitude) at the lateral occipital scalp sites (PO7/PO8) that were used to measure ERPs contralateral and ipsilateral to the red target and were also evident for target-present displays (**Fig. 3B**, middle). The ERPs elicited by target-present displays also contained peaks that resembled the typical P1 and N1 elicited by non-isoluminant lateral target stimuli (**Figs. 1 and 2**). Once activity driven by the overall luminance change was removed (by subtracting target-absent ERPs from target-present ERPs), the waveforms were nearly identical to the typical ERPs, except that the P1 and N1 were delayed by 40–50 milliseconds (in high-salience target blocks) because the target and background were isoluminant (**Fig. 3B**, bottom; see Wijers et al., 1997). The P1 and N1 were delayed even further when the salience of the target was reduced (in low-salience blocks).



As in Experiment 1, the ipsilateral peaks (high-salience P1: 175 ms; low-salience P1: 207 ms) trailed the contralateral peaks (high-salience P1: 138 ms; low-salience P1: 168 ms),  $t_s(11) \geq 3.52$ ,  $p_s \leq .005$ ,  $d_s \geq 1.63$ , as would be expected based on commissural transmission of sensory information from contralateral to ipsilateral occipital areas. N1 latencies were not quantified due to the absence of clear ipsilateral N1 peaks in some of the jackknifed sub-averages, but inspection of the grand averaged waveforms suggests that the ipsilateral N1 also lagged the much larger contralateral N1 by around 40 ms. In addition to these latency differences, the ipsilateral peaks were more positive than the contralateral peaks, beginning in the time range of the P1 (high-salience: 114  $\mu\text{V}^*\text{ms}$  vs. 51  $\mu\text{V}^*\text{ms}$ ; low-salience: 92  $\mu\text{V}$  vs. 50  $\mu\text{V}^*\text{ms}$ ),  $t_s(11) \geq 2.43$ ,  $p_s \leq .033$ ,  $d_s \geq 0.61$ , and continuing into the time range of the N1 (high-salience: -54\*ms  $\mu\text{V}$  vs. -202  $\mu\text{V}^*\text{ms}$ ; low-salience: -31  $\mu\text{V}^*\text{ms}$  vs. -166  $\mu\text{V}^*\text{ms}$ ),  $t_s(11) \geq 4.50$ ,  $p_s < .001$ ,  $d_s \geq 1.20$ .

Experiment 2 confirmed that it is possible to isolate the typical pattern of ERP activity driven by a lateral stimulus that appears against the background of a display-wide luminance change. However, it was not possible to isolate the VOA in Experiment 2 because no comparison of attend-target versus attend-elsewhere conditions was possible. Such a comparison was done in Experiment 3 using the new presentation method. Experiment 3 was similar to Experiment 1 but with a less noticeable stimulus change at fixation. Participants ( $N = 17$ ) discriminated the length of a salient red line (as in Experiment 2) that appeared to the left or right of fixation (attend-periphery condition) or monitored the fixation disc for a vertical notch that was one or three pixels deep (attend-fixation condition; **Fig. 4A**). In the attend-periphery condition, the occipital ERPs recorded contralaterally and ipsilaterally to the red line resembled the waveforms obtained in Experiment 2, with P1 and N1 peaks superimposed on deflections driven by the display-wide luminance change (**Fig. 4B**). The ipsilateral P1 was later and larger than the contralateral P1 [timing: 180 ms vs. 158 ms,  $t(16) = 2.76$ ,  $p = .014$ ,  $d = 1.79$ ; mean amplitudes over 150–250 ms: 283  $\mu\text{V}^*\text{ms}$  vs. 175  $\mu\text{V}^*\text{ms}$ ,  $t(16) = 5.44$ ,  $p < .001$ ,  $d = 1.68$ ]. No such amplitude difference was observed in the attend-fixation condition [ipsilateral P1: 217  $\mu\text{V}^*\text{ms}$ ; contralateral P1: 202  $\mu\text{V}^*\text{ms}$ ;  $t(16) = 1.19$ ,  $p = .250$ ,  $BF_{01} = 2.19$ ]. Comparing across conditions of Experiment 3, the ipsilateral P1 was significantly larger in the attend-periphery condition than in the attend-fixation condition,

$t(16) = 2.60$ ,  $p = .019$ ,  $d = 3.68$ . Although the contralateral N1 appeared to be larger in the attend-periphery condition (area over 225–275 ms:  $54 \mu\text{V}\cdot\text{ms}$ ) than in the attend-fixation condition ( $94 \mu\text{V}\cdot\text{ms}$ ), the difference was not significant,  $t = 1.24$ ,  $p = .232$ ,  $BF_{01} = 2.07$ .

To isolate and visualize the lateralized ERP differences associated with orienting, attend-fixation ERPs were subtracted from the corresponding attend-periphery ERPs. These between-condition difference waveforms contained a sustained positive difference over the ipsilateral scalp that began in the time range of the P1 (**Fig. 4C**). Topographical mapping revealed the occipital distribution of this ipsilateral positivity in the time range of the P1 (**Fig. 4D**). The mapping also showed that the contralateral negativity in the time range of the N1 seen in **Fig. 4C** had a maximal amplitude over the anterior scalp. A discrete regional source analysis over a 50-ms interval centered on the ipsilateral VOA (190–240 ms) revealed a source immediately adjacent to the lingual gyrus of the ipsilateral occipital cortex (Talairach coordinates:  $x = -20.1$ ,  $y = -72.6$ ,  $z = -12.5$ ; **Fig. 4E**). This single ipsilateral source accounted for over 93% of the activity within the VOA interval. The goodness of fit improved to over 97% with the addition of regional sources near contralateral occipital cortex ( $x = 23.5$ ,  $y = -85.7$ ,  $z = -18.9$ ) and frontal cortex ( $x = -7.9$ ,  $y = 65.9$ ,  $z = -2.2$ ). A PCA of the residual activity revealed no dominant principal component, and so no additional source was necessary. All in all, these findings buttress conclusions from Experiment 1 and confirm that visually guided orienting activity begins in the time range of the P1 under conditions where other salient stimuli (e.g., at fixation) do not engage attention momentarily. Moreover, the difference in timing of the VOA between Experiments 1 and 3 indicates that the orienting activity is at least partially separable from the visually evoked P1 and N1 components.

Thus far, we have attributed VOA to the visually guided orienting of attention. However, there is an alternative explanation: Narrowly focusing attention at fixation may have suppressed early cortical processing of the peripheral stimulus (Belopolsky and Theeuwes, 2010; Theeuwes, 2010). In particular, the P1 and N1 components are highly sensitive to such spatial attention manipulations (e.g., Mangun, 1995; Hillyard and Anllo-Vento, 1998; Di Russo et al., 2003). Consequently, the changes in the ipsilateral P1 and N1 amplitude across conditions may have been associated with suppression of these components in the attend-fixation condition rather

than with orienting in the attend-periphery condition. We tested this alternative explanation in the final two experiments by replacing the fixation conditions from Experiments 1 and 3 with new conditions that would discourage observers from orienting to a lateral stimulus without restricting the spatial extent of their attentional focus.

Experiment 4 was similar to Experiment 3, but instead of a uniform reduction in background luminance, the luminance dropped to slightly different values inside ( $20 \text{ cd/m}^2$ ) and outside ( $22 \text{ cd/m}^2$ ) of a circular region, thereby creating the perception of a faint, grey disc (**Fig. 5A**). The disc was so inconspicuous that most participants failed to see it at the beginning of the practice session. The salient red line from Experiments 2 and 3 was presented on every trial within the spatial confines of the faint disc. In different halves of the experiment, participants ( $N = 24$ ) discriminated between short and long lines (attend-line condition) or between small and large discs (attend-disc condition). We hypothesized that if the lateralized amplitude differences observed thus far are due to the visually guided orienting of attention, they should be evident in the attend-line condition and should be substantially reduced in the attend-disc condition. In addition, we presumed that spatial attention would be equally distributed across the display in the two conditions at the start of each trial, because, unlike in Experiments 1 and 3, there would be no need to narrowly focus attention in either condition. Consequently, orienting-related activity could be isolated by subtracting ERPs obtained in the attend-disc condition from the ERPs elicited by the identical display in the attend-line condition.

The lateral-occipital ERPs contained the same early negative deflection (peak latency  $\sim 70$  ms) that was seen in Experiments 2 and 3 as well as a positivity that peaked at  $\sim 110$  milliseconds (**Fig. 5B**). These were essentially identical in the two conditions and thus were driven by the display-wide luminance changes. Following those two earliest peaks, the waveforms were characterized mainly by an ipsilateral P1 peak that was substantially larger in the attend-line condition than in the attend-disc condition. The difference waveforms (attend-line condition minus attend-disc condition) contained two prominent peaks: an early, ipsilateral positivity that peaked roughly 180 ms post-stimulus (i.e., in the time range of the ipsilateral P1), and a larger, bilateral positivity that peaked 300–350 ms post-stimulus (**Figs. 5C**). The VOA was isolated by subtracting

the contralateral waveform from the ipsilateral waveform (**Fig. 5D**). This peak was statistically significant with respect to baseline (area over 100–250 ms:  $149 \mu\text{V}\cdot\text{ms}$ ; mean amplitude over 135–210 ms:  $1.7 \mu\text{V}$ ),  $p = .002$ ,  $d = 1.79$ , was larger on fast-response trials ( $207 \mu\text{V}\cdot\text{ms}$ ) than on slow-response trials ( $167 \mu\text{V}\cdot\text{ms}$ ; **Fig. 5E**),  $t(23) = 2.22$ ,  $p = .037$ ,  $d = 0.41$ , and preceded the onset of unrestrained saccades made in the direction of the target (VOA: 153 ms; saccade: 218 ms; **Fig. 5F**),  $t(23) = 9.28$ ,  $p < .001$ ,  $d = 2.43$ . The split-half reliability of the VOA was .81, which indicates that the process driving this scalp-recorded component occurred reliably across trials. Topographical mapping revealed that the VOA was seen primarily as a positive voltage over the ipsilateral scalp (**Fig. 5G**), although there was also a small contralateral negativity in the first phase of the VOA (150–200 ms).

Although the disc was barely perceptible in Experiment 4, there were still two abrupt-onset stimuli in the display. Thus, the VOA might possibly be associated with the competitive biasing of attention to one stimulus over another (Luck et al., 1997; Desimone, 1998). The purpose of Experiment 5 was to measure the VOA to a single isoluminant target line in the absence of a competing stimulus. Experiment 5 was similar to Experiment 4 except that the disc was darker, appeared in three sizes instead of two, and was absent on half of the trials (**Fig. 6A**). The attend-line-condition task was the same as before (short vs. long), whereas in the attend-disc-condition task, participants were asked to press one of two buttons to indicate the presence or absence of the disc. Notably, on disc-absent trials, the red line was the only abrupt-onset stimulus in the display.

**Figures 6B and 6C** show the lateral-occipital ERPs elicited by disc-absent and disc-present displays, respectively. Each panel contains ERPs obtained in the two conditions (attend-line and attend-disc), and the corresponding attend-line-minus-attend-disc differences are plotted in **Figs. 6D and 6E** (waveforms and topographical maps, respectively). The disc-present ERPs look different from those obtained in Experiment 4 due to the increased salience of the disc. However, the ipsilateral P1 was still substantially larger in the attend-line condition than in the attend-disc condition ( $246 \mu\text{V}\cdot\text{ms}$  vs.  $112 \mu\text{V}\cdot\text{ms}$ ; mean amplitudes measured 125–225 ms),  $t(23) = 4.27$ ,  $p < .001$ ,  $d = 0.70$ . The ERPs from disc-absent trials closely resemble the waveforms obtained in

Experiment 4, with an initial negative voltage that peaked at 70 milliseconds and a subsequent positive voltage that peaked at 110 milliseconds. Once again, the ipsilateral P1 was larger in the attend-line condition than in the attend-disc condition (200  $\mu\text{V}\cdot\text{ms}$  vs. 108  $\mu\text{V}\cdot\text{ms}$ ),  $t(23) = 3.80$ ,  $p < .001$ ,  $d = 0.69$ . A similar difference in the ipsilateral P1 was seen across conditions for disc-present displays (attend-line: 246  $\mu\text{V}\cdot\text{ms}$ ; attend-disc: 112  $\mu\text{V}\cdot\text{ms}$ ; **Fig. 6C**),  $t(23) = 4.27$ ,  $p < .001$ ,  $d = 0.70$ . In fact, the ipsilateral P1 was large in the attend-line condition but was essentially absent in the attend-disc condition. Critically, the attend-line minus attend-disc waveforms (**Fig. 6D**) and the topographical maps (**Fig. 6E**) show that the VOA was almost entirely a consequence of increased positivity over the ipsilateral occipital scalp, even in the complete absence of inter-stimulus competition (i.e., on disc-absent trials). The VOA was isolated by subtracting the contralateral waveform from the ipsilateral waveform (**Fig. 6F**) and its magnitude was found to be statistically significant on both disc-present trials (area over 100–250 ms: 192.7  $\mu\text{V}\cdot\text{ms}$ ; mean amplitude over 135–210 ms: 1.3  $\mu\text{V}\cdot\text{ms}$ ) and disc-absent trials (area: 136.1  $\mu\text{V}\cdot\text{ms}$ ; mean amplitude: 1.3  $\mu\text{V}\cdot\text{ms}$ ),  $ps = .002$ ,  $ds \geq 1.18$ .

## Discussion

An abrupt-onset visual stimulus appearing in an uncluttered visual field reflexively engages a covert orienting system that ultimately brings attention to bear upon the stimulated location (Posner, 1980; Posner and Petersen, 1990; Yantis and Jonides, 1990; Egeth and Yantis, 1997; Corbetta and Shulman, 2002; Carrasco, 2011). As a result, the sudden appearance of an irrelevant peripheral stimulus is known to affect the behavioral and neural responses to subsequent target stimuli. For example, salient peripheral cues modulate the amplitude of the P1 elicited by a subsequent target even when the cue is not predictive of the target's location (when the cue-target interval is sufficiently short; Eimer, 1994b; Hopfinger and Mangun, 1998; Hopfinger & Ries, 2005). Such peripheral-cueing effects are generally considered to result from the covert orienting of attention to the preceding cue, but there have been few attempts to identify and track the neural events associated with the visually guided covert orienting of attention that enables subsequent enhancement of target processing.

We investigated whether a specific neural correlate of the visually guided orienting of attention could be identified in ERP recordings. To distinguish orienting-related neural activity from purely sensory-evoked activity, ERPs elicited by a peripheral stimulus were compared under conditions of attention and inattention. These ERP recordings showed that the posterior-contralateral N1 component was not appreciably larger when participants attended to the eliciting peripheral stimulus than when they attended to a different stimulus, but the ipsilateral P1 and N1 peaks differed considerably across conditions. Specifically, the ipsilateral activity was more positive when the eliciting stimulus was attended than when it was unattended, starting in the time range of the P1 (Experiments 3–5) or the N1 when there was competition from fixation stimuli (Experiment 1). In these experiments the task-relevant peripheral stimulus had to be discriminated and thus required an orienting of attention to its location. Accordingly, the ipsilateral positivity associated with this orienting was designated *Visual Orienting Activity (VOA)*. Discrete regional source analyses indicated that the VOA reflects neural activity within or near the lingual gyrus of the ipsilateral occipital cortex.

The VOA evident in Experiments 4 and 5 cannot be ascribed to task-related differences in top-down spatial attention because observers needed to distribute their attention widely in both conditions (that is, there was no spatial restriction of the attentional focus that would suppress processing of stimuli at more peripheral locations). The VOA was larger on fast-response trials than on slow-response trials, was dissociable from overt orienting of the eyes (i.e., was not due to inadvertent saccadic eye movements), and was evident even when there was no other abrupt-onset stimulus in the display. Consequently, we conclude that the VOA reflects neural processes in occipital cortex associated with the covert orienting of attention to a lateral target stimulus rather than processes associated with purely sensory processing, overt orienting, or competitive biasing of attention over other stimuli in the visual field.

In theory, orienting-related ERP modulations could arise from excitatory processes in the contralateral visual cortex that guide attention to the location of the stimulus, from inhibitory processes in the ipsilateral visual cortex that prevent attention from inadvertently moving to the wrong hemifield, or from a mixture of excitatory and inhibitory processes. Although it appears that

the VOA reflects processes in the ipsilateral cortex, it is not entirely clear whether the VOA reflects attentional modulation of sensory-evoked activity in the ipsilateral hemisphere (e.g., increased amplitude of the ipsilateral P1 component) or separate, endogenous activity in the ipsilateral lobe that would otherwise be absent when an observer refrains from orienting attention. On the one hand, the VOA did occur reliably within the time range of the P1 and N1 peaks, suggesting that it might be a modulation of sensory-evoked componentry. This was the case even when the P1 and N1 peaks were delayed by the use of a novel stimulus presentation method (Experiments 2–5) and by a reduction of stimulus salience (Experiment 2). On the other hand, the precise timing of the VOA varied within the P1-N1 time range depending on the presence and salience of competing stimuli (e.g., at fixation) that might delay orienting. In either case, the VOA appears to be a reliable ERP signature of the visually guided orienting of attention.

Although the VOA occurs within the time range of the early visual ERP components, it can be distinguished conceptually and empirically from the many P1 attention modulations in the classic ERP studies of attention. Conceptually, these classic studies sought to determine how focusing attention on a particular region of space (or some other aspect of the environment) affects processing of stimuli appearing there or elsewhere (for reviews, see Hillyard & Anllo-Vento 1998; Mangun, 1995). The earliest of these studies used sustained attention paradigms to determine whether spatial selection occurs at an early or late stage of processing (e.g., Van Voorhis and Hillyard 1977; Hillyard and Mangun, 1988). Later studies used trial-by-trial cueing paradigms to determine whether focusing attention has similar consequences on stimulus processing under more dynamic conditions (Eimer, 1994a; Mangun and Hillyard, 1991). In contrast, the present study did not investigate how the spatial focusing of attention modulates processing of subsequent stimuli but rather sought to isolate ERP activity associated with the spatial orienting of attention itself. The lateral stimuli found to elicit the VOA were presented at locations that were unattended prior to stimulus onset. The presence or absence of VOA depended not on whether the stimulus appeared in an attended region of space but whether participants were required to orient attention to the stimulus once it appeared. Empirically, the vast majority of the classic studies of spatially focused attention (cited above) reported ERP

modulations over the contralateral scalp, whereas the VOA identified in the present study was localized to the ipsilateral scalp.

Although this is the first report of isolated ERP activity associated with visually guided orienting, the VOA was likely present (although not isolated) in several prior ERP studies. For example, one spatial-cueing study reported that a peripheral cue appearing to the left or right of fixation elicits an “early negative potential shift” over the contralateral occipital scalp in the time range of the P1 and N1 peaks (Yamaguchi et al., 1994). This lateralized ERP difference was interpreted to be an enhancement of the negative N1 component over the contralateral scalp and was surmised to result from a combination of purely sensory (“exogenous”) processes and attentional allocation in visual space. The present study confirms that part of the lateralized ERP difference reflects attentional allocation (i.e., covert orienting) in visual space but shows that this VOA is a positivity that occurs primarily in the ipsilateral visual cortex and is dissociable from the N1.

Other peripheral cueing studies compared ERPs elicited by visual targets that appeared at cued locations or at other (uncued) locations (here called valid-cue and invalid-cue trials, respectively). In such comparisons, the VOA might be evident on invalid-cue trials if attention must be re-oriented from the cued location to the target location. Results of at least one study are consistent with this possibility (Eimer, 1994b). Over the contralateral occipital scalp, the target-elicited P1 was similar on valid- and invalid-cue trials. Over the ipsilateral occipital scalp, the P1 was *larger* on invalid-cue trials than on valid-cue trials. Eimer (1994b) surmised that sensory refractoriness may have led to a reduction of P1 amplitude on valid-cue trials (i.e., when cue and target stimulated the same visual neurons), but the finding is also consistent with the re-orienting account above. In any case, the procedures of that study did not allow for the isolation of ERP activity specifically linked to attentional orienting.

Although its precise functional significance is yet to be determined, we surmise that the VOA reflects an early stage of spatial selection that is necessary for identification of visual objects. In terms of the sequence of processing stages that have been hypothesized to underlie object identification (Jannati et al., 2013, Figure 7), we propose the VOA to be situated



immediately after the computation of stimulus salience (indexed by the Ppc component) and before selective processes associated with stimulus identification (indexed by the sustained posterior contralateral negativity, SPCN, component). One possibility is that the VOA may reflect suppression of ipsilateral visual cortex activity that would help to prevent deployment of attention in the wrong direction. In line with this hypothesis, the VOA might represent neural activity associated with a suppressive process or a reduction of sensory-evoked activity as a result of such suppression (e.g., a blocking a negative potential in the ipsilateral hemisphere that would normally be evoked in the absence of orienting to the ipsilateral stimulus).

The VOA may be compared with an ERP component associated with the focusing of attention upon individual objects appearing in multi-item displays (such as those used to study visual search). This component, called the posterior contralateral N2 (N2pc), is observed as an amplitude difference between contralateral and ipsilateral occipital ERPs in the time range of the N2 peak (200–300 ms post stimulus; Luck and Hillyard, 1994a, 1994b; Luck et al., 1997; Luck, 2012). The N2pc has been hypothesized to reflect a spatial-filtering process that either suppresses irrelevant items in a display (Luck and Hillyard, 1994a; Luck et al., 1997; Luck, 2012) or enhances processing of the attended item (Eimer, 1996; Hickey et al., 2009; Tay et al., 2019). Presumably, such a filtering process would take place only after attention has been oriented to the location of the attended item, and thus one might expect the VOA to be evident at a shorter latency than the N2pc in visual search tasks. This has generally not been observed with EEG recordings, but MEG recordings show an early phase of the “M2pc” (the MEG equivalent to the N2pc) that was hypothesized to reflect attention orienting (Hopf et al., 2000). The VOA and N2pc differ not only in terms of their timing (with the VOA earlier than the N2pc) but also in terms of their scalp topographies: Whereas the VOA appears as an enhanced positivity over the ipsilateral scalp, the N2pc appears as an enhanced negativity over the contralateral scalp (Luck and Hillyard, 1994b).

While the VOA has not been observed in visual-search studies, no N2pc was evident in the present study (or in the ERPs reprinted in **Fig. 1**). There are two possible interpretations for these contrasting results. First, the VOA and N2pc might reflect categorically different attentional

processes that occur under different conditions (e.g., VOA with single-item displays and N2pc with multi-item displays). By this account, the processes driving the VOA (presumed to be associated with rapid orienting to a single item) would not be required for covert deployment of attention to a target in a visual search array with multiple items; for example, as proposed by Luck and Hillyard (1994b), the spatial filtering processes indexed by the N2pc would not be required for identification of a single stimulus in an uncluttered visual field (as in the present study). Second, the two components might reflect the same general class of attentional process whose timing depends on the amount of inter-item competition and other factors that affect the duration of the pre-attentive processing stage. Here, we have used the term “orienting” to describe the process hypothesized to drive the VOA, but one might instead use the term “spatial selection” to describe the processes hypothesized to drive both the VOA and the N2pc. Thus, while different spatial selection processes may be required for items that appear with and without competing items, it may not be necessary that they occur in succession.

Researchers have also reported an N1pc component that occurs at an intermediate latency between the VOA and the N2pc (Wascher and Beste, 2010). The N1pc is observed using hybrid methods that combine the use of multi-item displays from simple search tasks (with one stimulus on each side of fixation; Eimer, 1996) and the lateralized stimulation used in the present study. The contributions of orienting activity and purely sensory processing to the N1pc have yet to be systematically assessed. On the face of it, however, the intermediate timing of the N1pc under such hybrid presentation conditions is consistent with the view that the VOA, N1pc, and N2pc all reflect to some degree the orienting of attention (or spatial selection) and that the latencies of these nominally different components reflect the duration of pre-attentive processing required to localize the eliciting stimulus.

Finally, an ERP component called the distractor positivity ( $P_D$ ) has been associated with suppression of distractors rather than attentional selection of targets (Hickey et al., 2009; Gaspar and McDonald, 2014). The  $P_D$  is a positive deflection observed contralateral to salient distractors that accompany task-relevant targets, and its amplitude is associated with visual search performance (larger  $P_D$  on fast search trials than on slow search trials; Gaspar & McDonad, 2014)

as well as visual working memory capacity (larger  $P_D$  for high-capacity individuals than for low-capacity individuals; Gaspar et al., 2016). Whereas the  $P_D$  appears to reflect suppression of a potentially distracting stimulus when attention is directed elsewhere (e.g., towards a less salient target), the VOA observed here might reflect suppression of an empty visual hemifield when attention is to be directed towards an abrupt-onset stimulus on the other side of fixation. Although future work is necessary to elaborate on the precise neural process underpinning the VOA, the present results suggest that the VOA represents a specific index of orienting to an abruptly onsetting single stimulus in an uncluttered display.

**References**

- Belopolsky AV, Theeuwes J (2010) No capture outside the attentional window. *Vis. Res.* 50: 2543–2550.
- Bisley JW, Mirpour K, Arcizet F, Ong WS (2011) The role of the lateral intraparietal area in orienting attention and its implications for visual search. *Eur. J. Neurosci.* 33: 1982–1990.
- Boehnke SE, Munoz DP (2008) On the importance of the transient visual response in the superior colliculus. *Curr. Opin. Neurobiol.* 18: 544–551.
- Carrasco M (2011) Visual attention: the past 25 years. *Vision. Res.* 51: 1484–1525.
- Corbetta M, Shulman GL (2002) Control of goal-directed and stimulus-driven attention in the brain. *Nat. Rev. Neurosci.* 3: 201–215.
- Desimone R (1998) Visual attention mediated by biased competition in extrastriate visual cortex. *Philos. Trans. R. Soc. Lond. B. Biol. Sci.* 29: 1245–1255.
- Di Russo F, Martínez A, Hillyard SA (2003) Source analysis of event-related cortical activity during visuo-spatial attention. *Cereb. Cortex* 13: 486–499.
- Di Russo F, Martínez A, Sereno MI, Pitzalis S, Hillyard SA (2002) Cortical sources of the early components of the visual evoked potential. *Hum. Brain. Mapp.* 15: 95–111.
- Duhamel JR, Colby CL, Goldberg ME (1992) The updating of the representation of visual space in parietal cortex by intended eye movements. *Science* 255: 90–92.
- Egeth HE, Yantis S (1997) Visual attention: Control, representation, and time course. *Annu. Rev. Psychol.* 48: 269–297.
- Eimer M (1994a) “Sensory gating” as a mechanism for visuospatial orienting: Electrophysiological evidence from trial-by-trial cuing experiments. *Percept. Psychophys.* 55: 667–675.
- Eimer M (1994b) An ERP study on visual spatial priming with peripheral onsets. *Psychophysiol.* 31: 154–163.
- Eimer M (1996) The N2pc component as an indicator of attentional selectivity. *Electroencephalogr. Clin. Neurophysiol.* 99: 225–234.
- Gaspar JM, McDonald JJ (2014) Suppression of salient objects prevents distraction in visual search. *J. Neurosci.* 34: 5658–5666.

- Gaspar JM, Christie GJ, Prime DJ, Jolicœur P, McDonald JJ (2016) Inability to suppress salient distractors predicts low visual working memory capacity. *Proc. Natl. Acad. Sci. U. S. A.* 113: 3693–3698.
- Hatfield G (1998) Attention in early scientific psychology. in *Visual Attention* (Wright RD, ed) pp3–2. New York: Oxford UP.
- Hickey C, Di Lollo V, McDonald JJ (2009) Electrophysiological indices of target and distractor processing in visual search. *J. Cogn. Neurosci.* 21: 760–775.
- Hillyard SA, Anllo-Vento L (1998) Event-related brain potentials in the study of visual selective attention. *Proc. Natl. Acad. Sci. U. S. A.* 95: 781–787.
- Hopf JM et al (2000) Neural sources of focused attention in visual search. *Cereb. Cortex* 10: 1233–1241.
- Hopfinger JB, Mangun GR (1998) Reflexive attention modulates processing of visual stimuli in human extrastriate cortex. *Psychol. Sci.* 9: 441–447.
- Hopfinger JB, Ries AJ (2005) Automatic versus contingent mechanisms of sensory-driven neural biasing and reflexive attention. *J. Cogn. Neurosci.* 17: 1341–1352.
- Ives HE (1912) Studies in the photometry of lights of different colors. *The London, Edinburgh, and Dublin Philosophical Magazine and Journal of Science* 24: 149–188.
- James W (1890) *Principles of Psychology*. New York: Dover.
- Jannati A, Gaspar JM, McDonald JJ (2013) Tracking target and distractor processing in fixed-feature visual search: evidence from human electrophysiology. *J. Exper. Psychol. Hum. Percept. Perform.* 39: 1713–1730.
- Johannes S, Munte TF, Heinze HJ, Mangun GR (1995) Luminance and spatial attention effects on early visual processing. *Brain. Res. Cogn. Brain. Res.* 2: 189–205.
- LaBerge D (1995) *Attentional processing: The brain's art of mindfulness*. Harvard University Press.
- Luck SJ (2012) Electrophysiological correlates of the focusing of attention within complex visual scenes: N2pc and related ERP components. in *The Oxford handbook of event-related potential components* (Luck SJ, Kappenman ES, eds) pp329–360. New York: Oxford UP.

- Luck SJ, Girelli M, McDermott MT, Ford MA (1997) Bridging the gap between monkey neurophysiology and human perception: an ambiguity resolution theory of visual selective attention. *Cogn. Psychol.* 33: 64–87.
- Luck SJ, Hillyard SA (1994a) Spatial filtering during visual search: evidence from human electrophysiology. *J. Exper. Psychol. Hum. Percept. Perform.* 20: 1000–1014.
- Luck SJ, Hillyard SA (1994b) Electrophysiological correlates of feature analysis during visual search. *Psychophysiology* 31: 291–308.
- Mangun GR (1995) Neural mechanisms of visual selective attention. *Psychophysiology* 32: 4–18.
- Mangun GR, Hillyard SA (1988) Spatial gradients of visual attention: behavioral and electrophysiological evidence. *Electroenceph. Clin. Neurophysiol.* 70: 417–428.
- Mangun GR, Hillyard SA (1991) Modulations of sensory-evoked brain potentials indicate changes in perceptual processing during visual-spatial priming. *J. Exper. Psychol. Hum. Percept. Perform.* 17: 1057–1074.
- Marino RA, Rodgers CK, Levy R, Munoz DP (2008) Spatial relationships of visuomotor transformations in the superior colliculus map. *J. of Neurophysiol.* 100: 2564–2576.
- McDonald JJ, Green JJ, Jannati A, Di Lollo V (2013) On the electrophysiological evidence for the capture of visual attention. *J. Exper. Psychol. Hum. Percept. Perform.* 39: 849–860.
- Miller J, Patterson T, Ulrich R (1998) Jackknife-based method for measuring LRP onset latency differences. *Psychophysiol.* 35: 99–115.
- Perrin F, Pernier J, Bertrand O, Echallier JF (1989) Spherical splines for scalp potential and current density mapping. *Electroencephalogr. Clin. Neurophysiol.* 72: 184–187.
- Phipson B, Smyth GK (2010) Permutation P-values should never be zero: Calculating exact P-values when permutations are randomly drawn. *Stat. Appl. Genet. Mol. Biol.* 9.
- Posner MI (1980). Orienting of attention. *Quart. J. Exper. Psychol.* 32: 3–25.
- Posner MI, Petersen SE (1990) The attention system of the human brain. *Annu. Rev. Neurosci.* 13: 25–42.
- Rodgers CK, Munoz DP, Scott SH, Paré M (2006) Discharge properties of monkey tectoreticular neurons. *J. Neurophysiol.* 95: 3502–3511.

- Rouder JN, Speckman PL, Sun D, Morey RD, Iverson G. (2009) Bayesian t tests for accepting and rejecting the null hypothesis. *Psychon. Bull. Rev.* 16: 225–237.
- Rugg MD, Lines CR, Milner AD (1984) Visual evoked potentials to lateralized visual stimuli and the measurement of interhemispheric transmission time. *Neuropsychologia* 22: 215–225.
- Saron CD, Davidson RJ (1989) Visual evoked potential measures of interhemispheric transfer time in humans. *Behav. Neurosci.* 103: 1115–1138.
- Sawaki R, Geng JJ, Luck SJ (2012) A common neural mechanism for preventing and terminating the allocation of attention. *J. Neurosci.* 32: 10725–10736.
- Stoermer VS, McDonald JJ, Hillyard SA (2019) Involuntary orienting of attention to sight or sound relies on similar neural biasing mechanisms in early visual processing. *Neuropsychologia* 132: 107122.
- Tay D, Harms V, Hillyard SA, McDonald JJ (2019) Electrophysiological correlates of visual singleton detection. *Psychophysiol.* 56: e13375.
- Tay D, Jannati A, Green JJ, McDonald JJ (2022) Dynamic inhibitory control prevents salience-driven capture of visual attention. *J. Exper. Psychol. Hum. Percept. Perform.* 48: 37–51.
- Theeuwes J (2010) Top–down and bottom–up control of visual selection. *Acta Psychologica* 135: 77–99.
- Van Voorhis S, Hillyard SA (1977) Visual evoked potentials and selective attention to points in space. *Percept. Psychophys.* 22: 54–62.
- Wascher E, Beste C (2010) Tuning perceptual competition. *J. Neurophysiol.* 103: 1057–1065.
- Wijers AA, Lange JJ, Mulder G, Mulder LJ (1997) An ERP study of visual spatial attention and letter target detection for isoluminant and nonisoluminant stimuli. *Psychophysiology* 34: 553–565.
- Wurtz RH, Goldberg ME (1972) Activity of superior colliculus in behaving monkey. 3. Cells discharging before eye movements. *J. Neurophysiol.* 35: 575–586.
- Yamaguchi S, Tsuchiya H, Kobayashi S (1994) Electroencephalographic activity associated with shifts of visuospatial attention. *Brain* 117: 553–562.

Yantis S, Jonides J (1984) Abrupt visual onsets and selective attention: evidence from visual search. *J. Exp. Psychol. Hum. Percept. Perform.* 10: 601–621.

Yantis S, Jonides J (1990) Abrupt visual onsets and selective attention: voluntary versus automatic allocation. *J. Exper. Psychol. Hum. Percept. Perform.* 16: 121–134.



**Figure Captions**

**Fig. 1.** Prototypical ERPs elicited by a visual stimulus appearing abruptly to the left or right side of fixation in an otherwise empty field. By convention, ERPs are collapsed across left and right fields and left and right occipital electrodes to reveal waveforms recorded contralaterally and ipsilaterally with respect to stimulus lateralization. Figure adapted with permission from Luck and Hillyard (1994b, Fig. 6).

**Fig. 2.** Experiment 1 methods and results. **(A)** Example trial sequence and stimulus display. **(B)** Grand-average ERPs elicited by the red disc, recorded over the contralateral and ipsilateral occipital scalp (electrodes PO7/PO8) in the attend-periphery condition (left) and the attend-fixation condition (right). The horizontal dashed line indicates  $-4 \mu\text{V}$ . Negative voltages are plotted upward. **(C)** Attend-periphery-minus-attend-fixation difference waveforms recorded contralaterally and ipsilaterally to the disc. The shaded region is centered on the initial positive peak in the ipsilateral waveform and is designated as Visual Orienting Activity (VOA). **(D)** Topographical voltage map of the attend-periphery minus attend-fixation difference amplitude averaged over the 150–190-ms time window (shaded region in part C). **(E)** A single regional source (Talairach coordinates:  $x = -32.6$ ,  $y = -76.7$ ,  $z = -4.2$ ) localized to the ipsilateral lingual gyrus accounted for over 90% of scalp-recorded activity in the 150–190-ms modeling interval. The ipsilateral and contralateral cerebral hemispheres correspond to the left and right sides of the image, respectively.

**Fig. 3.** Experiment 2 methods and results. **(A)** Example trial sequence and stimulus display. **(B)** Grand-averaged occipital ERPs elicited by target displays containing no red line (target absent), a high-salience red line, or a low-salience red line. ERPs elicited by the lateral red lines were isolated by subtracting target-absent ERPs from target-present ERPs. Activity triggered by the display-wide luminance change (including N68 and P106) is evident in target-present and target-absent waveforms but is removed from the difference waveform. **(C)** Topographical maps of the difference waves shown in panel B. The left and right sides of the head correspond to the ipsilateral and contralateral scalp, respectively.

**Fig. 4.** Method and results from Experiment 3. **(A)** Trial sequence showing change in background luminance, red line, and notched fixation disc on target display. **(B)** Grand-average occipital ERPs elicited by the target display in the two conditions. **(C)** Attend-periphery minus attend-fixation difference waveforms recorded contralaterally and ipsilaterally with respect to the line. **(D)** Topographical voltage maps of the average attend-periphery-minus-attend-fixation difference within the 175–275-ms time window.

**Fig. 5.** Methods and results from Experiment 4. **(A)** Example trial sequence. **(B)** Grand-average occipital ERPs elicited by the target display in the two conditions. **(C)** Difference waves created by subtracting the attend-disc condition ERPs from the attend-line condition ERPs. Neural activity associated with putatively “pure” sensory processing, including the early negative peak associated with the display-wide luminance change, is removed from the difference waves, leaving activities associated with task-specific attentional processes. The waveforms reveal visual orienting activity (VOA; shaded in red) associated with the orienting of attention to the red line. **(D)** Ipsilateral-minus-contralateral difference wave corresponding to the isolated waveforms in panel C, with 95% CIs (vertical red bars). The vertical dashed line indicates the time point at which VOA reached 50% of its peak amplitude. **(E)** Ipsilateral-minus-contralateral difference wave from panel D separately plotted for fast- and slow-response trials based on the median reaction times. **(F)** Activity elicited by unrestrained horizontal saccades to the abrupt-onset line in the attend-line condition. The vertical dashed line indicates the time point at which this saccadic activity reached 50% of its peak amplitude. **(G)** Topographical maps of the VOA. The left and right sides of the heads correspond to the ipsilateral and contralateral scalp, respectively.

**Fig. 6.** Methods and results from Experiment 5. **(A)** Example trial sequence. **(B)** Grand-averaged occipital ERPs elicited by disc-present displays across the two conditions. **(C)** Grand-averaged occipital ERPs elicited by disc-absent displays across the two conditions. **(D)** Difference waves created by subtracting the attend-disc-condition ERPs from the attend-line-condition ERPs, revealing the VOA (shaded in red). **(E)** Topographical maps of the VOA. The left and right sides of the heads correspond to the ipsilateral and contralateral scalp, respectively. **(F)** Ipsilateral-

minus-contralateral difference waves corresponding to the isolated waveforms in panel D, with 95% CIs (vertical red bars).

Fig. 1.

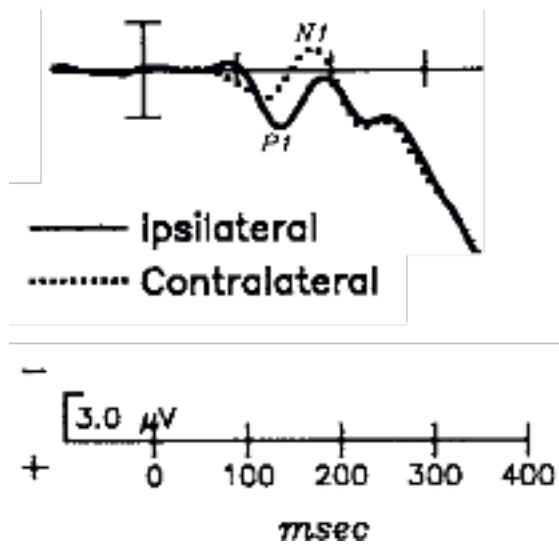
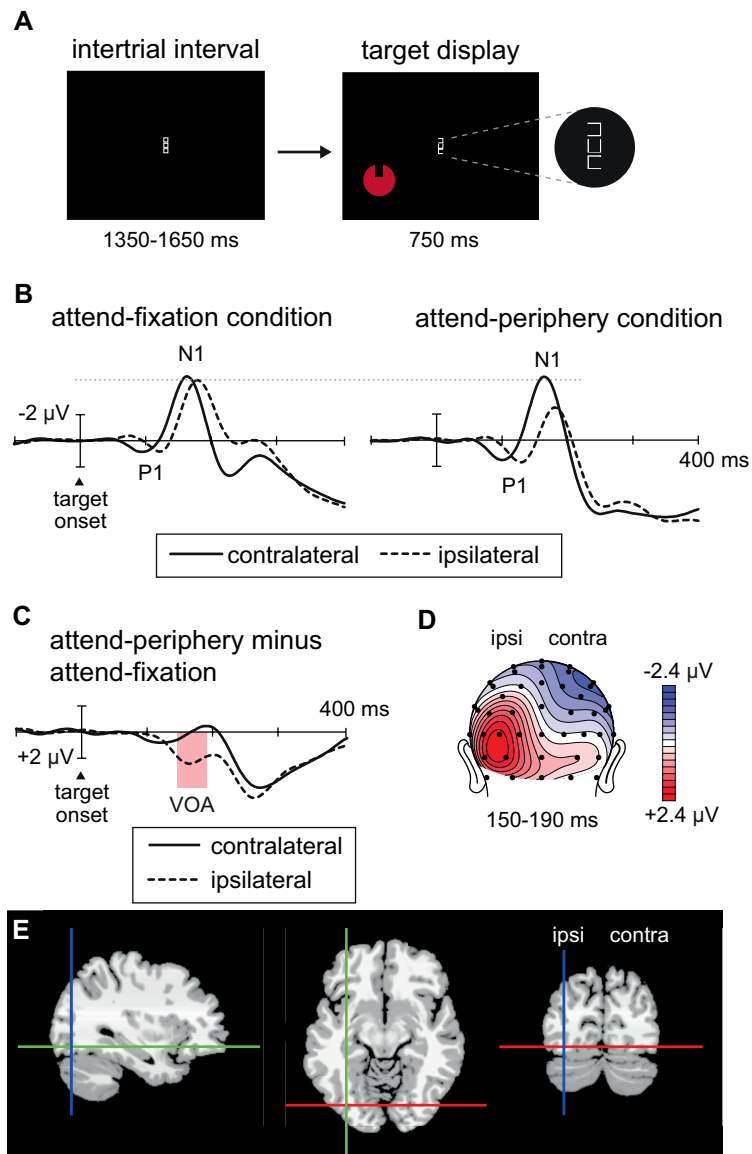
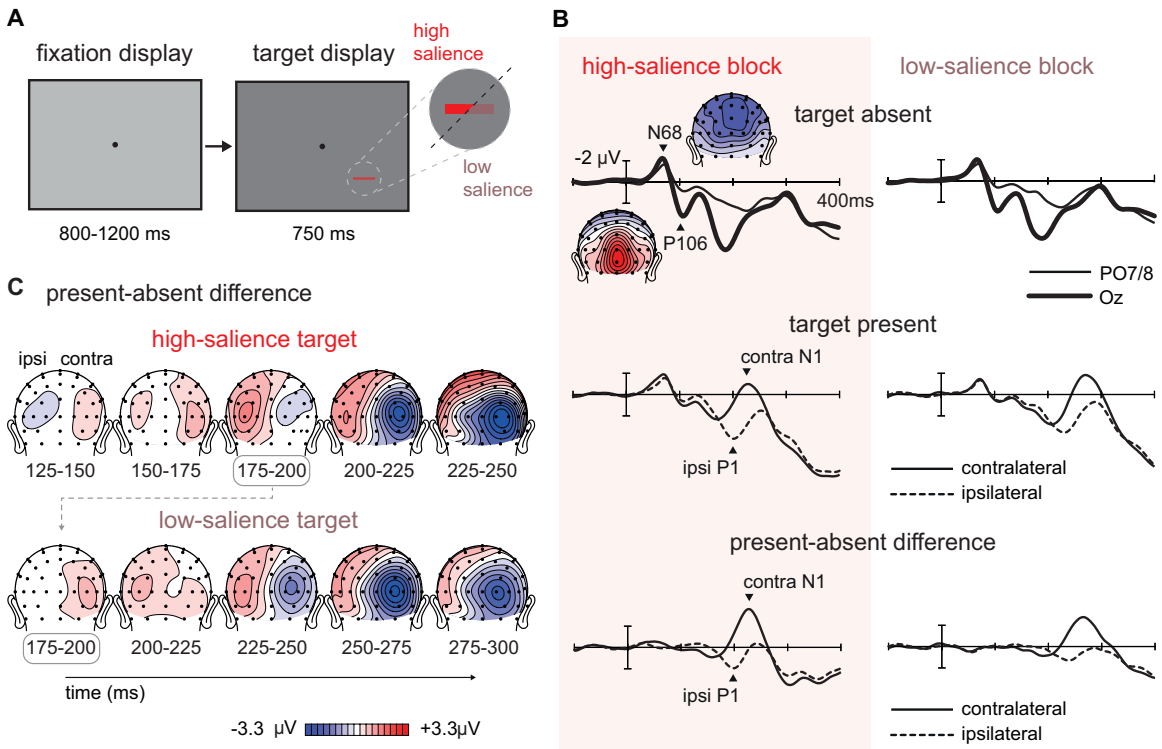


Fig. 2.



**Fig. 3.**



**Fig. 4.**

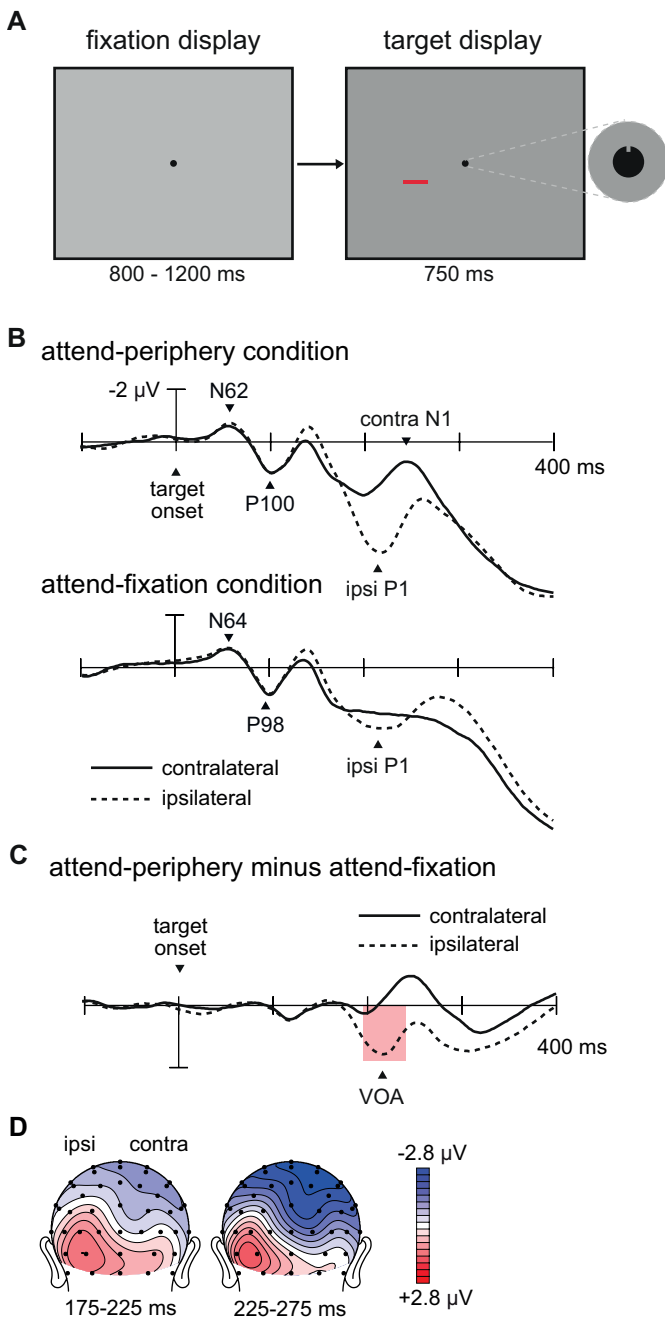


**Fig. 5.**

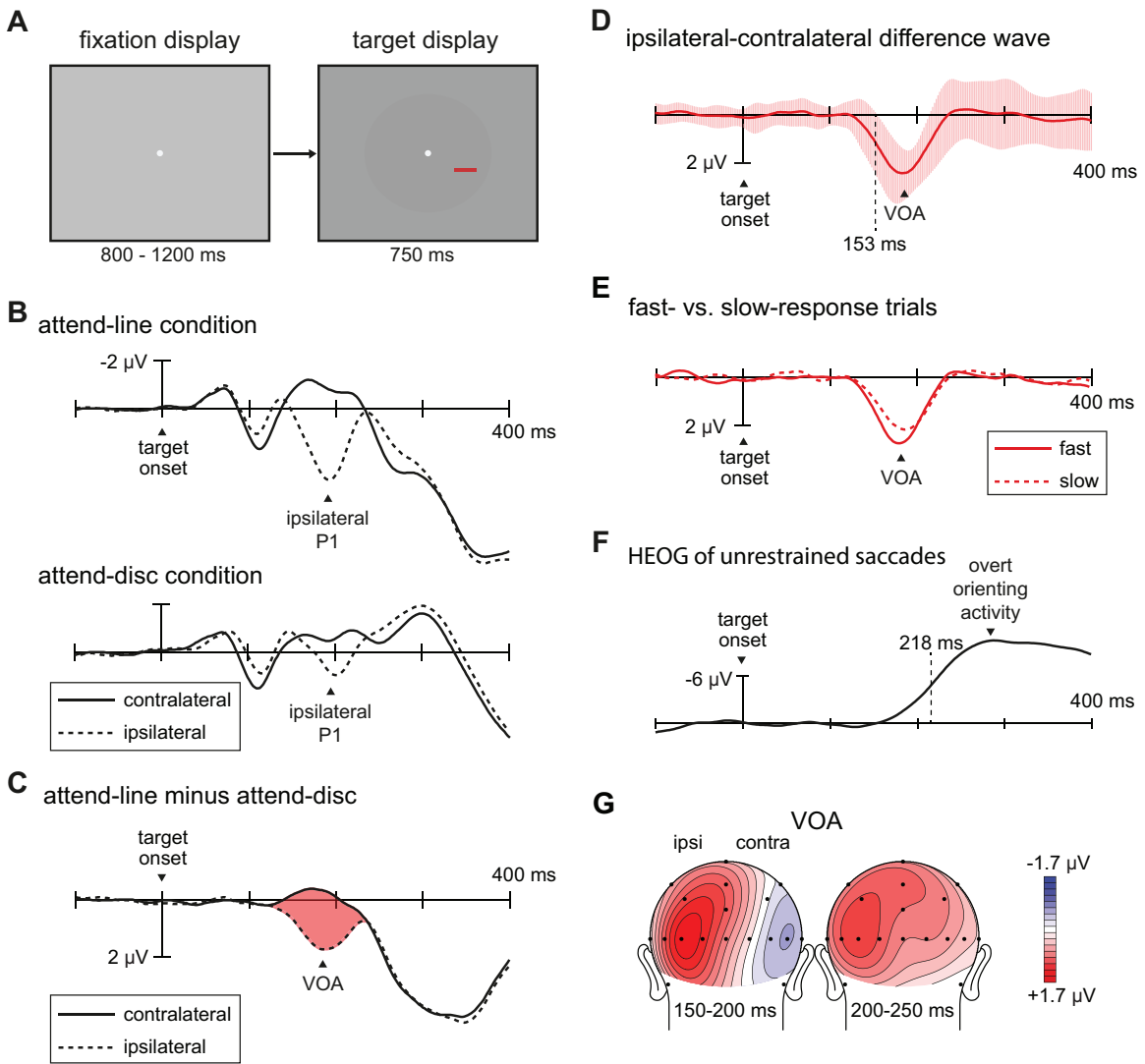




**Fig. 6.**

